Hydro-Oceano & Sedimentation Model of Brondong Lamongan Harbour

Moch Thufail Basyarahil[1], *Rizqi* Abdi Perdanawati[1] , *M. Yunan* Fahmi[1*]

1 Department of Marine Science , Faculty of Science and Technology, Sunan Ampel State Islamic University, Surabaya, Indonesia

Abstract. PPN Brondong in East Java is a vital fisheries hub, catching around 200 tonnes of fish in a day and serving as an export hub. To maintain port efficiency and properly manage vessel activities, hydro-oceanographic modelling is important. This research uses a quantitative approach with primary and secondary data analysis. Using Delft3D, this study modelled the currents and sedimentation in PPN Brondong for one year, covering the east and west monsoons. The results show a diurnal tidal pattern, with dominant winds from the east in the east monsoon and west in the west monsoon. Peak waves reached 1.6 metres in the west monsoon and 0.9 metres in the east monsoon. The maximum current velocity of 0.23 m/s occurred in the west monsoon. TSS was higher in the west monsoon, reaching 1kg/m3. Erosion and sedimentation differed between monsoons; steady erosion occurred in shallow areas and sedimentation in deeper areas. The eastern harbour basin is prone to erosion due to high currents, while the western part experiences sedimentation. This research provides in depth understanding for sustainable harbour management at PPN Brondong.

1 Introduction

The Brondong Nusantara Fishing Port (PPN) of East Java is a Class B fishing port with a catch of around 200 tonnes per day, capable of serving regional and national fishing vessels. The catch is exported to various countries, including Thailand, the Netherlands, Italy, France, the United Kingdom, Belgium, the United States, Spain, Malaysia, and other countries. Ministry detailed that in 2018 the PPN Brondong Lamongan in East Java received 10744 vessel visits with 971 fishing boats, and 9731 fishermen. This shows that PPN Brondong Lamongan East Java is the centre of the community's economy [1].

Development in coastal areas results in sedimentation impacts, such as in research at Patimban port which explains that after the construction there was sedimentation of 6.06 cm/year after the construction of the port in Patimban waters [2]. Research in Jakarta Bay also increased sedimentation after the reclamation island which caused the current around the Port to weaken, the weakened current caused the concentration of sediment deposition to

* Corresponding author:: myunanf@gmail.com

increase. The initial condition before reclamation had a sediment concentration of $5.61\text{x}10^{-8}$ kg/m^2/s while after reclamation the sediment concentration increased to $1.33\text{x}10^{-7}$ kg/m^2/s [3].

Considering the importance of the PPN Brondong in Lamongan, East Java, which is the centre of the community's economy, it is necessary to pay attention to the needs of the port in order to make good use of the port function and not affect ship-to-ship activities. The government usually dredges the harbour channel [4]. Hydro-Oceanographic modelling is an alternative to determine the current and sedimentation patterns that occur in the PPN Brondong, by considering observational data that matches the actual conditions at the PPN Brondong. Based on the results of modelling analysis, it can be seen that sediment deposits are located in the PPN Brondong Lamongan, this can become data and management of dredging planning management for the PPN Brondong Lamongan in East Java.

2 Literature Review

Modelling is the process of constructing a simplified mathematical reality. In the process, numerical methods or models are often used to explain in more detail complex physical realities [5]. Hydrodynamic models are mathematical representations of fluid movement, such as water or air flow, that consider various factors such as pressure, velocity, viscosity, and mass distribution in the fluid system to predict flow patterns [6]. The flow hydrodynamics model in the software uses the continuity equation and momentum equation [7].

Continuity equation :

$$\frac{\partial h}{\partial t} + \frac{\partial \underline{u}}{\partial x} + \frac{\partial \underline{v}}{\partial y} = hs \qquad (1)$$

(Source : Manual, 2020)

Momentum equation :

$$\frac{\partial h\underline{u}}{\partial t} + \frac{\partial h\underline{u}^2}{\partial x} + \frac{\partial h\underline{v}\underline{u}}{\partial y} = f\underline{v}h - gh\frac{\partial \eta}{\partial x} - \frac{h}{\rho_0}\frac{\partial p_a}{\partial x} - \frac{gh^2}{2\rho_0}\frac{\partial \rho}{\partial x} + \frac{\tau_{sx}}{\rho_0} + \frac{\tau_{bx}}{\rho_0} - \frac{1}{\rho_0}\left(\frac{\partial s_{xx}}{\partial x} + \frac{\partial s_{xy}}{\partial y}\right) + \frac{\partial}{\partial x}(hT_{xx}) + \frac{\partial}{\partial y}\left(hT_{xy}\right) + hu_sS \qquad (2)$$

$$\frac{\partial h\underline{v}}{\partial t} + \frac{\partial h\underline{v}^2}{\partial x} + \frac{\partial h\underline{v}\underline{u}}{\partial y} = -f\underline{u}h - gh\frac{\partial \eta}{\partial y} - \frac{h}{\rho_0}\frac{\partial p_a}{\partial y} - \frac{gh^2}{2\rho_0}\frac{\partial \rho}{\partial y} + \frac{\tau_{sx}}{\rho_0} + \frac{\tau_{bx}}{\rho_0} - \frac{1}{\rho_0}\left(\frac{\partial s_{yx}}{\partial x} + \frac{\partial s_{yy}}{\partial y}\right) + \frac{\partial}{\partial x}\left(hT_{xy}\right) + \frac{\partial}{\partial y}\left(hT_{yy}\right) + hv_sS \qquad (3)$$

In which:

t	: Time.
x, y	: Cartesian coordinates.
η	: Sea level.
d	: Depth of water.
h	: (η + h)
u, v	: Zonal and meridional and vertical current velocity components.
f	: The choriolis component (2Ω sin φ) where Ω is the Earth's rotational speed and φ is the latitudinal position.

g	: The acceleration of the Earth's gravitational force.
ρ	: Water density
S_{xx}, S_{xy}, S_{yx} & S_{yy}	: Radiation of water mass pressure tensor in components xx, xy, yx and yy.
vt	: Vertical turbulence.
Pa	: Air pressure
ρ0	: Water density reference.
S	: Discharge from source.
U_s & V_s	: Current speed of zonal and meridional components when entering the system

(Source : Manual, 2020)

3 Methods

3.1 Research Time And Location

This study was conducted during two monsoons, namely the East and West monsoons. The East monsoon runs from April - September 2022, while the West monsoon occurs from October 2022 - March 2023. This research was conducted at PPN Brondong, which is located in Lamongan Regency, East Java Province, Indonesia.

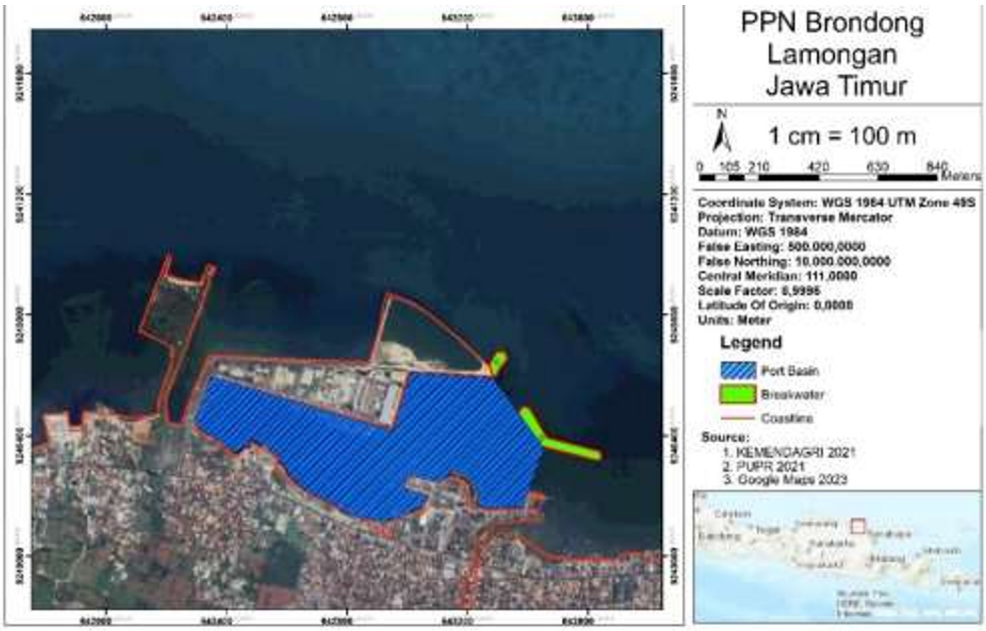

Fig 1. Research Area PPN Brondong Lamongan

3.2 Data

This research is a quantitative research with primary data analysis obtained from the Ministry of PUPR (Public Works and Housing) used as the main data source and some secondary data such as wind data from ERA-5, and tidal data from BIG station. The data was then processed and modelled using Delft3D software. Delft3D software was used to process and model the data obtained in detail to gain a better understanding of the phenomena being studied in the waters of the PPN Brondong Lamongan. The data used in modeling and its sources are presented in Table 1.

Table 1. Research Data.

No	Data	Sumber
1	Bathymetry Data	Deflt Dashboard 2022 dan PUPR 2021
2	Tidal Constant Data	Deflt Dashboard 2022
3	Sediment Data	PUPR 2021
4	Wind Data	ECMWF 2018-2022
5	River Discharge Data	PUPR 2021
6	Tidal Data	BIG 2022
7	Wave Data	ECMWF 2018-2022

River discharge data around PPN Brondong is used to support modelling, the data is very important because the largest TSS output is the river, there are two river data obtained, namely the Bengawan solo river and Kaliasinan river. more details can be seen in Table 2.

Table 2. Data on River Discharge and TSS of Rivers Around PPN Brondong.

River	River Flow m3/s		Cohesive Sediments kg/m3		Width (m)
	Monsoon		Monsoon		
	East	West	East	West	
Kaliasinan	2.635	28.56	0.02771	0.02771	17
Bengawan Solo	26.35	285.6	0.2771	0.2771	170

Source : PUPR, 2021.

3.3 Delft3D Model Simulation

Hydrodynamics (flow) modelling simulations use the continuity equation which means that the amount of water entering an area must be equal to the amount of water leaving the area, this equation is to understand how water flows and moves within a water area. The continuity equation is integrated with the momentum equation to understand how water moves, changes direction, and interacts with other things such as beaches or other objects in the water. The combination of these equations can develop a mathematical model that describes how ocean currents move and change from one location to another within a water domain.

Hydrodynamics (flow) simulation will be supported by (wave) simulation, because ocean waves affect ocean currents and vice versa, when waves collide with current they can change the speed and direction of the currents, and conversely ocean currents can also affect wave characteristics, such as wave height and length. Waves and currents both affect the transport of materials in the ocean, such as sediment from one location to another. The basic

mathematical principle of wave calculation uses Newton's law of motion, which explains that the change in water velocity is proportional to the force exerted on it. When the wind force exerts a push on the water surface, waves are formed due to this change in velocity. Hooke's principle is applied in terms of a restorative force that seeks to return water to its equilibrium position proportional to the displacement from the equilibrium position itself. This means that when water is pushed from its equilibrium position, the restorative force seeks to return it to its original position [8].

The modelling simulation time period is 1 year, then divided into two monsoons, namely the east and west monsoons, where the east monsoon is represented by August 2022 and the west monsoon in December 2022 which has the most extreme conditions. The morphological scale value was changed to 6 to represent 1 month of modelling as 6 months. There are two kinds of grids used that use UTM WGS84 coordinate references. A large grid of the modelling area in order to produce a more even distribution of wind energy throughout the modelling area, and the interaction of waves with the topographic conditions of the seabed which can then affect the pattern and size of the waves generated. A detailed grid is required to capture the specific conditions of the surrounding environment, such as rivers, beaches or offshore structures. The grid is then combined using the NESTHD method in order to obtain computational results that are closest to the actual conditions in the PPN Brondong area.

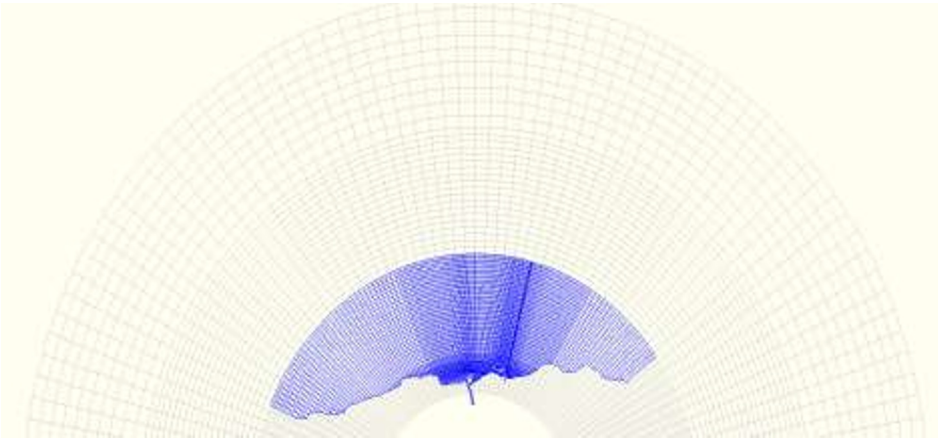

Fig 2. Large Grid and Detail Grid.

3.4 Bathymetry and Boundary Conditions

Bathymetry is the study of measuring the depth of the ocean, sea or other body of water. Bathymetry map is a map that describes waters and their depth [9]. The bathymetry data used in this study is secondary data obtained from PUPR in 2021. Bathymetry maps are needed to gain a better understanding of the topographic characteristics of the seabed and how it affects the flow of currents and tides. Bathymetry is very important to estimate the interaction between tides and water topography including the formation of turbulence, river flow, or changes in current patterns during high or low tides [10].

Boundary conditions are intended to define modelling boundaries using the .bnd format, where tidal constant values are entered at each predefined boundary. In this case the boundary values are determined directly in the modelling, the boundary conditions use the astronomic component constraints by entering the tidal constant values. In the detailed grid, the boundary conditions use time series data obtained from the nesting of large grids. Utilisation of specific time series data can provide a more detailed and realistic calculation

of tidal variations at a smaller scale. River discharge and TSS data were also input using total discharge type boundary conditions. The total discharge type was used at the modelling boundary to include data on water discharge and sediment content of the river in time series.

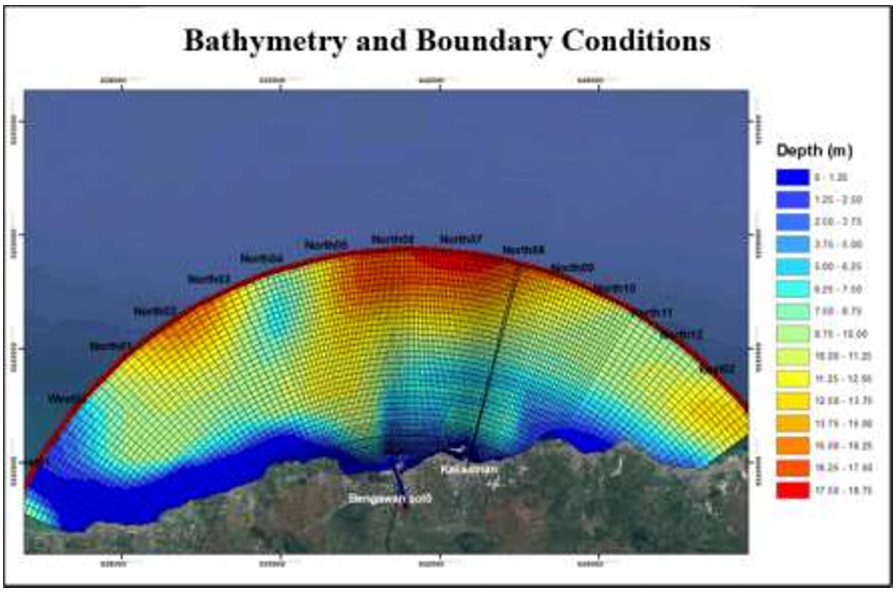

Fig 3. Bathymetry and Boundary Conditions.

3.5 Tidal Data Processing

Tidal data for modelling validation uses secondary data from BIG, so that the modelling can be confirmed. Tidal data were collected at the BIG station with coordinates 06° 51 52.02 N and 112° 22 6.528 E for 30 days from 1 to 30 August 2022 with measurement time every 1 hour. The tidal data were then analysed using the Least Squere method to produce tidal harmonic constants with magnitudes in the form of amplitude (A) and phase (g°) in each component, the data are listed in Table 3.

Table 3. Harmonic Components and Important Terms of the Tides.

	O1	P1	K1	N2	M2	S2	K2	M4	MS4
A (m)	0.2533	0.1697	0.5074	0.0171	0.0577	0.0398	0.0268	0.0001	0.0001
g (˚)	317.5377	17.2750	256.5832	261.7180	84.2681	342.2106	187.0602	296.8102	266.7938

Unsur	Hitungan	Hasil	Satuan
S0	Z0+1.1(M2+S2)	0.107	m
HAT	Z0+(all constituents)	1.072	
HHWL	Z0+(M2+S2+N2+K1+O1+P1)	1.045	
HWS	Z0+(M2+S2+K1+O1)	0.858	
MHWL	Z0+(M2+K1+O1)	0.818	
Z0	MSL	0	
MLWL	Z0-(M2+K1+O1)	-0.818	
LWS	Z0-(M2+S2+K1+O1)	-0.858	
LLWL	Z0-(M2+S2+N2+K1+O1+P1)	-1.045	
LAT	Z0-(all constituents)	-1.072	
F	(O1+K1)/(M2+S2)	7.804	

Source: BIG Station 2022.

Formzahl number is a number that has a certain range used to determine the tidal type of an area, using Formzahl number, the calculation of the harmonic component is used to determine the tidal characteristics [11]. The tidal elevation calculated by the Least Square method is classified as a diurnal type, with one high tide and one low tide occurring in one day with an F value of 7.804. The results of this calculation are reinforced by Prahmadana's research in 2013 where tidal data taken from fifteen days of tidal surveys at the location of PPN Brondong on 12 July 2012 onwards, have a single diurnal tidal type [12].

3.6 Wind Data Processing

Wind data is very important in the modelling process because wind has a major impact on the movement of current direction and speed, becoming an important factor in the formation of current patterns [13]. Wind has a significant impact on wave formation at sea. Waves at sea can be divided into several types depending on the source of generation, one of which is wind waves, which are formed due to wind blowing that produces friction between air and water surfaces. The height and period of the waves generated are influenced by the wind speed (U), wind duration (D), fetch (F), and wind direction. The longer and stronger wind blows, the larger waves formed, illustrating the close relationship between wind conditions and the characteristics of ocean waves formed [14]

Wind and wave distribution is presented in the form of rose diagrams, the presentation of wind data in the form of coloured rose diagrams, where the display is adjusted to the interval of wind speed and direction according to field conditions, will make the information easier to understand [15]. Wind and wave data were obtained from ECMWF and then processed using WRPLOT. The rose diagram displays the frequency distribution of events from each direction and interval of wind speed and wave height that has been determined for a specific date and period. Data processing was carried out for the last 10 years (2013 – 2022).

The east monsoon has a dominant wind direction coming from the east with a frequency of 32.4%, the wind distribution in the east monsoon is dominated by speeds in the range of 3 - 4 m / s with a frequency value of 29.9%. The speed value of more than 5 m/s has a distribution value of 7.8% and the speed of 0 - 1 m/s has a relatively small frequency of 3.4%. In the west monsoon the dominant wind direction comes from the west which has a frequency of 31.6%, with the dominance of speed in the range of 2 -3m/s which has a frequency value of 25.7%. The west monsoon has a speed frequency value of more than 5 m/s which is greater than the east monsoon with a frequency of 12.9%, wind speed data in the form of a rose diagram can be seen in Fig 4.

The east monsoon wave data is dominated from the east which has a very dominant frequency with a value of 89.9%, the eastern monsoon wave height which has the greatest frequency is the wave with a height between 0 - 1m with a frequency of 61.7%. In the east monsoon the waves tend to be calmer which only has a maximum wave height with a value in the range of 1.5 - 2m and only has a very small distribution frequency of 0.06%. The west monsoon waves are dominated from the northwest with a frequency of 54.9%, in the west monsoon it has a wave height value of more than 2m with a frequency of 0.6%, and there is a wave height value in the range of 1.5 - 2m with a frequency of 3.1%.

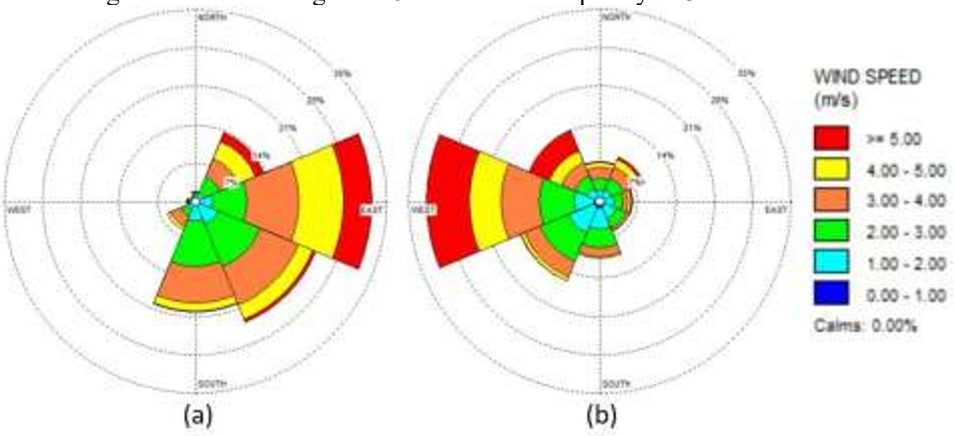

Fig 4. Wind Rose Diagram (a) East Monsoon (b) West Monsoon.

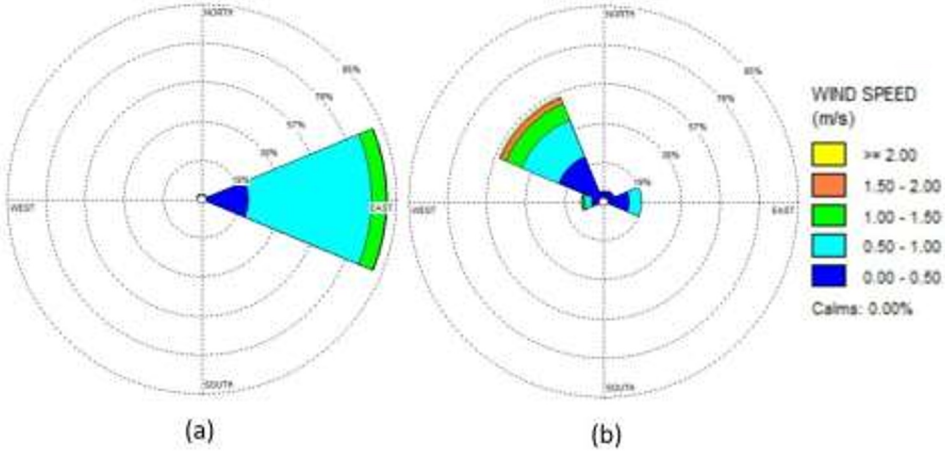

Fig 5. Wave Rose Diagram (a) East Monsoon (b) West Monsoon.

3.7 Model Validation

Model validation is very important to determine the suitability between data obtained from the model and directly observed data, this is to evaluate the extent to which the model is able to approach the actual conditions, despite the limitations in the flow input boundary conditions and the data entered. Validation of the modelling results was carried out by comparing secondary tidal data obtained from the Geospatial Information Agency (BIG) and secondary wave data from ERA-5 observed with the results obtained from the model. The

goal is to assess the accuracy of the model, if the smaller RMSE (Root Mean Square Error) value indicates a relatively small error rate of the modelling results [16].

The results of secondary data analysis with modelling results in the waters of PPN Brondong Lamongan show very low RMSE values, namely 0.081465 for tides and 0.05 for waves. This indicates a high level of prediction accuracy in the modelling data. The tidal and wave prediction results from the modelling can be effectively utilised for subsequent processes, particularly in current and sediment modelling.

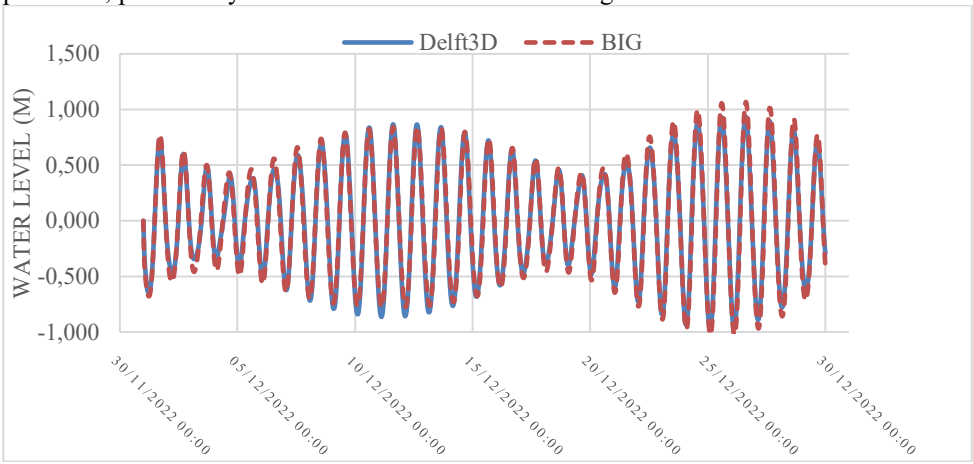

Fig 6. Tidal Validation.

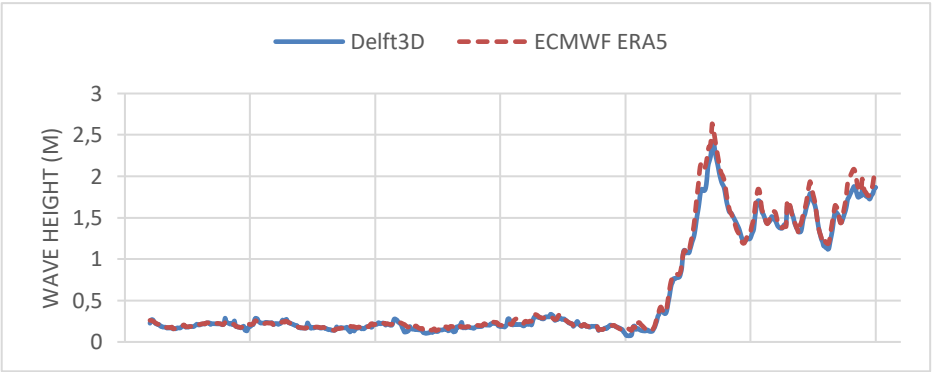

Fig 7. Wave Validation.

4 Results and Discussion

4.1 Wave Model

In the ocean, there are various waves with different causes and restoring forces. In the context of marine meteorology, the three types of waves based on their generating forces are wind-induced waves, earthquakes (tsunamis), and tidal waves triggered by the gravitational pull between the earth, moon and sun. Wind-driven waves dominate in terms of occurrence and the energy they carry over the sea surface [17]. Surface waves are often caused by wind over the water surface. The nature of waves reaching the shore is strongly influenced by the depth of the sea and the contours of the shore, as well as the characteristics and parameters of the waves themselves. The journey of waves towards the shore undergoes significant changes,

influenced by environmental factors such as water depth and the shape of the beach profile [18].

The results of wave modelling in the waters of the PPN Brondong Lamongan show that in the east monsoon the highest waves have a value of 0.9 m, this is because in the east monsoon the wind blows predominantly with a speed of 3 - 4m / s and only a few winds have a speed of more than 5m / s, indicating that the east monsoon has relatively calm waves, in contrast to the west monsoon which has ocean waves reaching the highest height of 1.6m. This is due to the incidence of wind speeds exceeding 5 metres per second, which accounted for a large percentage of the 12.9%. This creates more choppy and dangerous sea conditions during the monsoon. Wave heights in the berth area are relatively smaller, as there is a breakwater before entering the berth area, where the wave height is only 0.1m. Waves are also influenced by bathymetry depth, which can be observed from the decrease in wave height as they approach the shoreline due to the change in bathymetry depth which tends to be shallower nearer the shore.

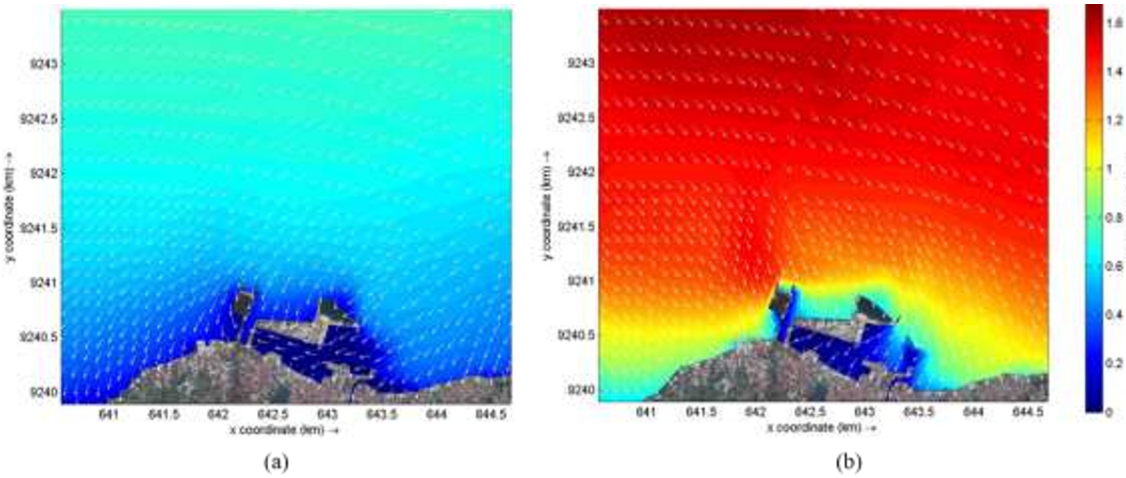

Fig 8. Significant Wave Height Modelling PPN Brondong (a) East Monsoon (b) West Monsoon.

4.2 Current Model

Ocean currents are defined as the horizontal movement of water masses in the ocean triggered by various driving forces, such as tides, wind pressure, atmospheric pressure differences, and ocean waves [19]. In general, ocean currents can be categorised into four main types. Firstly, currents associated with the density distribution of seawater, where density differences cause water movement. Second, tidal currents, which are caused by the gravitational forces of the Moon and Sun and periodic changes in sea level. Thirdly, currents arising from ocean waves, which produce horizontal water movement. Lastly, currents arise due to the influence of wind, where wind pressure moves masses of seawater horizontally [20].

The condition of the east monsoon currents towards the tide can be seen in Fig 9, when heading towards the eastern monsoon tide in PPN Brondong is dominated by currents heading westward, this is in accordance with the Eastern monsoon wind data where the dominant wind direction comes from the east towards the west, the wind has an influence on the movement of current direction and speed. In the condition towards the tide is also accompanied by the movement of the current towards the land, because when the tide is approaching its peak, seawater tends to flow towards the coast because of the stronger gravitational pull of the Moon and the Sun that pulls seawater towards the land. The current

speed at the time of the eastern high tide in the open sea area has a speed of 0.1 m/s to 0.15 m/s. The current tends to slow down when it reaches the harbour area, and the speed decreases further when it is in the berth area 0.01 m/s - 0.05 m/s, the magnitude of the current speed can be reduced due to the presence of breakwaters, the current speed transmitted by the waves will be slower because the wave energy has been reduced. This process can also reduce the strength of the underwater currents affected by the waves [21].

The direction at low tide of the current is dominated to the north, this indicates a very large influence by tides on the current. The current velocity during low tide conditions ranges from 0.05 m/s - 0.15 m/s, the maximum current velocity occurs in the Kaliasianan River area reaching 0.3 m/s. Different from the condition towards the tide which has a greater current speed in the open sea area, the condition towards the low tide has a large current speed in the beach area and will decrease when it reaches the open sea, the direction of the current when the condition towards the low tide is very dominant away from the coastline, namely towards the north. at the time of the highest tide current conditions will tend to weaken because the water mass towards the coast. At low tide, the water mass moves outside the shoreline, resulting in a larger current [22].

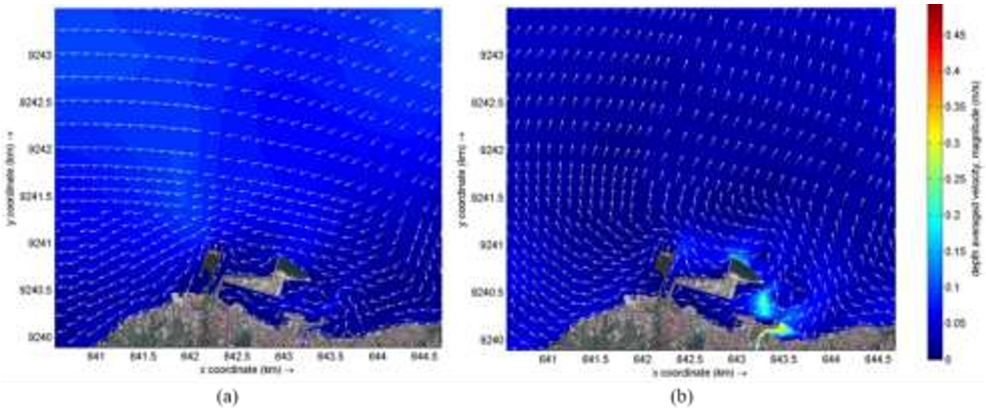

Fig 9. East Monsoon Current Pattern Towards (a) High Tide (b) Low Tide.

Western monsoon modelling in PPN Brondong Lamongan current towards the tide is presented in Fig 10. At the time of the tide the current is dominated towards the west with a speed range of 0.01 m/s - 0.15 m/s. The direction of the current at the time of the tide tends to be the same between the east and west monsoons, which means that in the waters of the PPN Brondong, the tides play a greater role in the formation of current patterns. The currents generated by the tides are very dominant in the process of rotation of water masses in coastal waters [23]. In the west monsoon the currents tend to have a greater speed than the east monsoon currents, because the speed and direction of surface currents can be influenced by the wind, because the wind in the west monsoon is dominantly greater, the current speed is also high [24].

Modelling results at low tide the current is dominated towards the northeast with a speed range of 0.1 m/s - 0.23 m/s. The speed of the current towards the ebb during the west monsoon is relatively high, because it is influenced by wind and tides that reinforce each other. When heading to low tide, the current speed increases due to the influence of tides, and is strengthened by the large wind speed during the monsoon. In the Kaliasinan river area, the current speed reaches 1 m/s, this is because in the western monsoon the river water discharge is quite high reaching 28.56 m3/s. The speed of the river current is influenced by the river water discharge, the greater the river water discharge, the greater the current [25]. Conditions in the west season tend to have larger currents referring to the results of research by Saputra

in 2017 based on current measurement data in the field showing currents in Surabaya waters have a maximum speed of 0.71 m / s in the west season and 0.7 m / s in the east season [26].

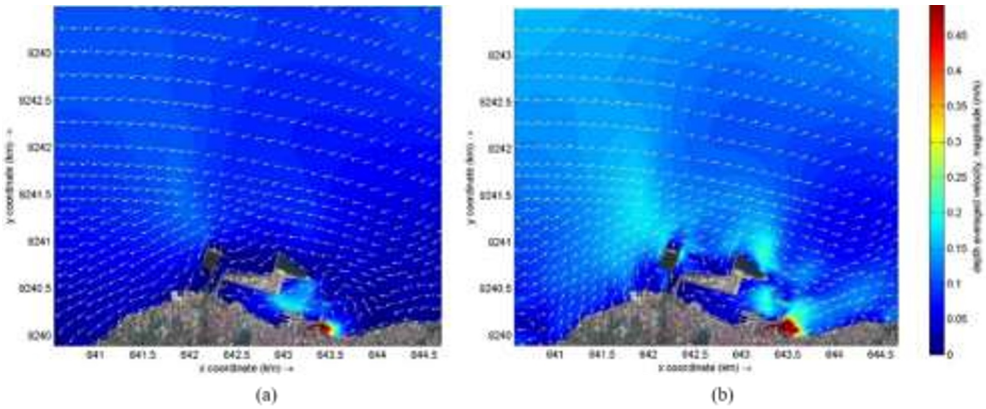

Fig 10. West Monsoon Current Pattern Towards (a) High Tide (b) Low Tide.

4.3 TSS Model

The distribution of TSS in the ocean is strongly influenced by the strength of currents and waves as they are the main factors that affect the movement of solid particles in the water. Strong ocean currents can transport TSS from river mouths, eroded coastal areas or construction sites into the water. Strong currents can carry TSS to deeper areas of the ocean or move it away from its source, depending on the direction and speed of the current [27]. Ocean waves also play an important role in TSS dispersal. Waves can break solid particles into smaller sizes and agitate seawater, allowing TSS to be dispersed more evenly across the ocean surface. In addition, waves can also affect TSS transport to shore or away from shore depending on the direction and strength of the waves [28]. In the east monsoon maximum TSS at the study site has a value of 0.01 kg/m^3, this is because in the east monsoon the currents and waves are relatively calmer, as a result TSS particles tend not to be stirred up and spread evenly throughout the water area, resulting in a lower maximum value of TSS distribution.

The results of the western monsoon TSS distribution model, showed that the maximum TSS at the study site had a value of 0.02 kg/m3. In the west monsoon, the concentration of TSS distribution is greater because it has a large wave height and current speed, supported by high discharge and TSS content in the river around the study area. The main source of sediment in the ocean is sediment from rivers. The process of erosion on land produces sediment particles such as sand, silt, soil and organic matter. River water carries these particles to estuaries and eventually to the sea. Rivers carry sediments from various sources such as mountains, plateaus, slopes and eroded land surfaces. These sediments are then carried by the river flow to the estuary and then dispersed in the sea [29].

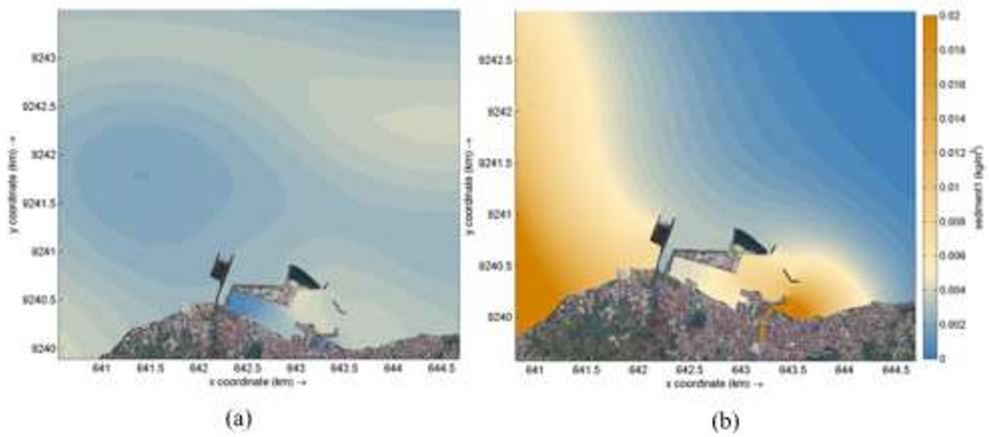

Fig 11. TSS Distribution (a) East Monsoon (b) West Monsoon.

4.4 Accumulation of Sedimentation and Erosion

Sedimentation occurs where solid particles in water or other fluids settle or settle to the bottom of a container or surface. This process occurs when the particles have a higher density than the medium in which they are located, so they tend to fall down due to gravitational forces [30]. Some factors that affect sedimentation are particle size, larger particles tend to have faster sedimentation rates than smaller particles. This is due to differences in volume surface relationships. Particle density plays an important role in determining sedimentation. Particles with higher density will have a greater gravitational force acting on them, so they will settle faster [31].

During the eastern monsoon, significant erosion occurred in the area near the Harbour, characterised by a decrease of -0.01m, while along the berth area, a sedimentation phenomenon occurred with an increase in height of 0.05m. The most striking sedimentation occurred to the east of the Harbour, reaching 0.15m. This indicates a high level of sedimentation especially in the port basin area, port basin area is a berth or parking area for ships can be seen in Fig 1, indicating the need for regular maintenance to maintain the smooth running of the harbour activities. Excessive sedimentation can result in navigation problems, such as insufficient depth for vessels to berth, as well as affecting accessibility to the harbour.

The west monsoon period is not too different from the east monsoon in terms of erosion in the area near the Harbour, with a value of 0.01m, and sedimentation phenomena in the berth area also occur. The difference lies in the west monsoon which displays a more even distribution of sedimentation, reaching a maximum value of 0.08m. This is due to the greater strength of currents and waves during the western monsoon, which results in the stirring up of sediments from the seabed and river sources, so that their distribution becomes wider and more evenly distributed in the waters. The deposition of sediment in the harbour pond area during each rainy season is due to the relatively small currents in the area. Calm currents can affect sedimentation. Calm currents tend to have low velocities or almost no flow at all, conditions like this cause sediment particles such as sand, mud, or organic material carried by seawater to have less energy to stay afloat or move. As a result, these sediment particles will tend to settle and be deposited at the bottom of the water [32].

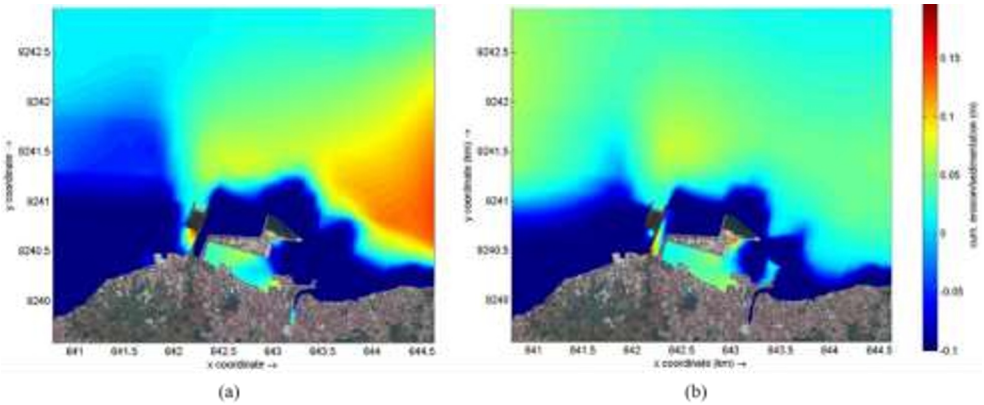

Fig 12. Accumulation of Sedimentation and Erosion (a) East Monsoon (b) West Monsoon.

4.5 Morphological Changes

Morphological change data in the Port area is displayed in the form of cross-sections that visualise changes in underwater bathymetry from the initial seabed elevation data to after one year of modelling. This cross-section data is for monitoring changes in underwater conditions in the Port area, so as to identify morphological changes that can affect ship loading and unloading activities and maintain safety and smooth operations at the port. crosssection location is shown in Fig 13.

Fig 13. Crossection Location.

The crosssection graph illustrates the comparison of the initial bed level elevation and the bed level elevation after 1 year. The comparison data is to facilitate the analysis of depth changes over one year of modelling. From the analysis of cross sections 1, 2 and 3, it can be seen that there is a similar pattern of seabed morphological change. At shallow depths, erosion tends to be stable with values between 0.1 and 0.3 metres, while at deeper depths

sedimentation processes occur with stable values ranging from 0.1 to 0.3 metres. This indicates a relative balance between erosion and sedimentation at the study site, suggesting that the most important factors stirring up sediments that cause sedimentation or erosion, namely currents and waves, are not too extreme. Sediment that follows the motion of current or wave patterns is called sediment transport. Sediment transport occurs due to the force of gravity on the sediment and the movement of the fluid that transports the sediment. The movement of sediments is influenced by the gravitational force of the earth that forms naturally and is assisted by the movement of water fluids contained in the sediment waters [33]. Currents and waves in the study area do not appear to create sediment transport conditions that lead to drastic changes in seafloor morphology, allowing erosion and sedimentation processes to take place in a more controlled manner.

Crossection 4 follows the horizontal direction of the shoreline, so its depth varies between 0.2 to 0.7 metres without significant difference. Although there was no significant difference in depth, crossection 4 experienced sedimentation and erosion. In the area of the western anchorage pond, there is a tendency for sedimentation because the value of current velocity is relatively small, such conditions cause sediment particles such as sand and mud carried by seawater to have less energy to stay afloat or move. As a result, these sediment particles will tend to settle. In the eastern part of the port basin area adjacent to the breakwater, erosion occurs due to higher current velocities. This location is influenced by stronger ocean currents because it is close to the open sea. These currents erode the shallow depth of the area, causing the area to erode. Sediment eroded in this area will fall on areas that have calm currents, namely in the western port basin area, so it can be said that the western port basin area is very vulnerable to sedimentation.

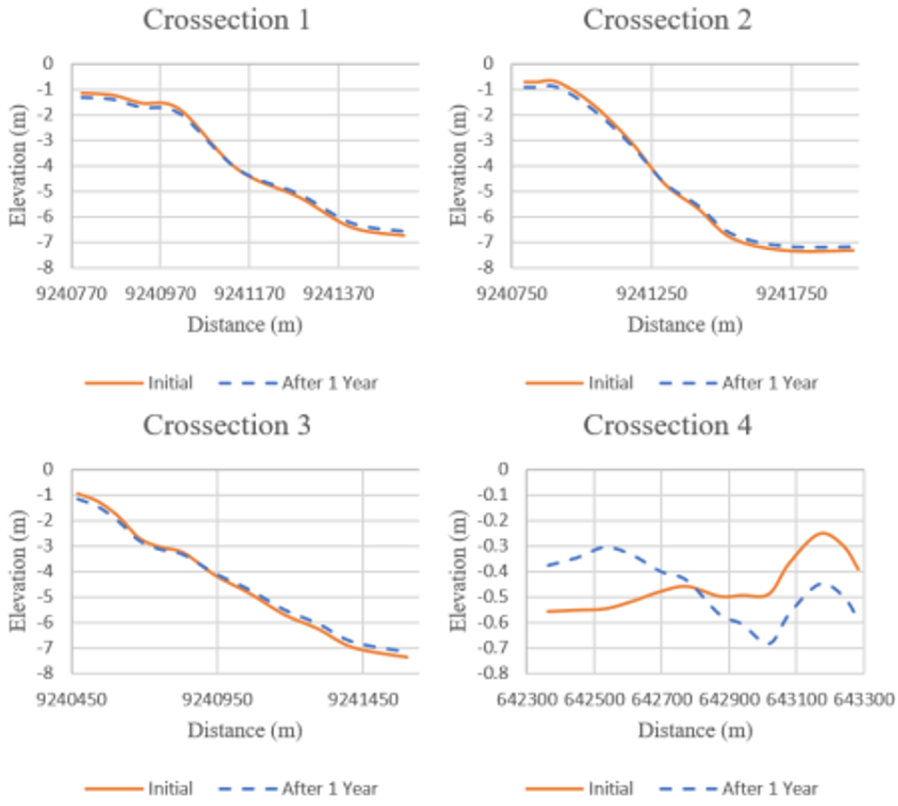

Fig 14. Morphological Change Chart.

5 CONCLUSIONS

The hydro-oceanographic model of the PPN Brondong Lamongan shows a diurnal tidal pattern, with one tidal cycle and one ebb cycle each day. Wind distribution tends to be dominant from the east in the east monsoon and from the west in the west monsoon. Waves in the study area are not very high, the peak wave recorded in the west monsoon reaches 1.6 metres, while in the east monsoon it is only about 0.9 metres. Current velocity is relatively calm with a maximum of 0.23 m/s occurring in the west monsoon, while current direction differs depending on the monsoon. TSS values showed differences between the east and west monsoons, with higher values in the west monsoon reaching 1kg/m3 due to the dominance of stronger currents and waves. Erosion and sedimentation phenomena occur in both monsoons, with the west monsoon showing a more even distribution of sedimentation, compared to the east monsoon which is more concentrated in the eastern area of the harbour. Morphological changes in crossections 1, 2 and 3 show a similar pattern, with stable erosion in the shallow areas within a range of 0.1 metres, while sedimentation occurs at deeper depths. The eastern harbour area, close to the breakwater, is prone to erosion due to high current velocities, while the western harbour area tends to experience sedimentation due to calmer currents, mainly due to sediments eroded from eroded areas.

BIBLIOGRAPHY

1. Kementrian, K. dan P. D. J. P. T. Profil PPN Berondong. in (2018). https://kkp.go.id/ancomponent/media/upload-gambar-pendukung/PPN Brondong/Profil Pelabuhan/PROFILPPNBRONDONG2018
2. Wibowo, M. Study of Sedimentation in the Water of Patimban Port Development Plan Using Computation Modeling. *J. Kelaut. Nas.* **1**, (2018). https://doi.org/10.15578/jkn.v1i1.6270
3. Saputra, R. A. PEMODELAN SEDIMENTASI PASCA REKLAMASI DAN MASTERPLAN DI TELUK JAKARTA MENGGUNAKAN PERANGKAT LUNAK MIKE. at http://digilib.uinsby.ac.id/26688/6/Rachmat Agung Saputra_H94214027.pdf (2018). http://digilib.uinsby.ac.id/26688/6/Rachmat Agung Saputra_H94214027
4. Tambunan Bestari, F. Y., Buana Sumanta, N. G. I. & Nur Iqbal, H. Model pengembangan infrastruktur pelabuhan perikanan. studi kasus pelabuhan perikananan nusantara brondong. *J. Tek. ITS* **10**, E85–E92 (2021).
5. Lee Barbour, S. & Krahn, J. Numerical Modelling Prediction or Process. *Geotech. News* **22.4**, 44–52 (2004). https://citeseerx.ist.psu.edu/document?repid=rep1&type=pdf&doi=38cc5506648a67f3d43c230ed345035a540dd423
6. Martí, J. M. & Müller, E. Numerical Hydrodynamics in Special Relativity Living Reviews in Relativity Article Amendments. *Living Rev. Relativ.* **6**, 1–100 (2003). http://www.mpagarching.mpg.de/hydro/index.shtmlhttp://relativity.livingreviews.org/lrr-2003-7http://www.livingreviews.org/lrr-2003-7/
7. Manual, U. *Delft3D 3D/2D Modelling Suite for Integral Water Solutions Hydro-Morphodynamics*. (2020).
8. Maleika, W. The influence of the grid resolution on the accuracy of the digital terrain model used in seabed modeling. *Mar. Geophys. Res.* **36**, 35–44 (2015). https://link.springer.com/content/pdf/10.1007/s11001-014-9236-6
9. Elok Dyah Kusumawati, Gentur Handoyo, H. PEMETAAN BATIMETRI UNTUK

MENDUKUNG ALUR PELAYARAN DI PERAIRAN BANJARMASIN, KALIMANTAN SELATAN. **4**, 706–712 (2015). http://ejournal-s1.undip.ac.id/index.php/jose

10. Utami, W. T. & P, D. G. Effect of Seabed Topography on Ocean Current Movement. *Geoid* **5**, 059–065 (2010).
11. Fadilah, Suripin & Sasongko, D. P. Menentukan Tipe Pasang Surut dan Muka Air Rencana Perairan Laut Kabupaten Bengkulu Tengah Menggunakan Metode Admiralty. **6**, 1–12 (2014).
12. Prahmadana, F., Armono, H. D. & Sujantoko. Pemodelan Gelombang di Kolam Pelabuhan Perikanan Nusantara Brondong. *J. Tek. POMITS* **2**, 150–154 (2013).
13. Kusumawati, I. Pemodelan Dinamika Arus Perairan Indonesia Yang Disebabkan Oleh Angin. *J. Perikan. Trop.* **3**, 1–10 (2016). https://doi.org/10.35308/jpt.v3i1.31
14. Triatmodjo, B. *Teknik Pantai*. (Beta Offset, 1999).
15. Fadholi, A., Pangkalpinang, S. M., Bandara, J., Amir, D. & Pinang, P. Analisis Data Arah Dan Kecepatan Angin Landas Pacu (Runway) Menggunakan Aplikasi Windrose Plot (Wrplot). *J. Ilmu Komput.* **9**, 84–91 (2013). http://www.wcc.nrcs.usda.gov
16. Candrasari, K., Rifai, A. & Handoyo, G. Peramalan Nilai Msl Berdasarkan Data Pasang Surut dengan Metode Admiralty dan Autoregressive Integrated Moving Average (Arima) di Perairan Pulau Pari Kepulauan Seribu. *J. Oseanografi* **4**, 28–34 (2015).
17. Triatmodjo, B. *Teknik Pantai (Ed, 2).* (Beta Offset., Yogyakarta, 1999).
18. Arianty, N., Mudin, Y. & Rahman, A. Pemodelan Refraksi Gelombang dan Analisis Karakteristik Gelombang Laut Di Perairan Teluk Palu Nova. *Gravitasi* **16**, 9–15 (2017).
19. Hadi, S. & Radjawane, I. *Arus Laut. Institut Teknologi Bandung Press* (2011).
20. Ippen, A. T. *Estuary and Coastline Hydrodynamics*. (McGraw-Hill Book Company, IncCatalog Card Number 65-27677, United States of America, 1966).
21. Alfarisi, A. & Suciaty, F. Perubahan Pola Hidrodinamika dan Sedimentasi Akibat Adanya Breakwater Di Pantai Glayem. 19–30 (2021).
22. Nugraha, R. B. A. & Surbakti, H. SIMULASI POLA ARUS DUA DIMENSI DI PERAIRAN TELUK PELABUHAN RATU PADA BULAN SEPTEMBER 2OO4. *J. Kelaut. Nas.* **4**, 48–55 (2009).
23. Sverdrup, K. A., Duxbury, A. & Duxbury., A. C. *Fundamentals of Oceanography*. (McGraw Hill Companies, New York, 2002).
24. Pamungkas, A. Karakteristik Parameter Oseanografi (Pasang-Surut , Arus , dan Gelombang) di Perairan Utara dan Selatan Pulau Bangka Abstract Characteristics of Oceanographic Parameters (Tidal , Flow , and Waves) in North and South of Bangka Island Bangka Belitung se. *Bul. Oseanografi Mar.* **7**, 51–58 (2018).
25. Myson, H. KAJIAN POTENSI ARUS SUNGAI LAGAN DI DESA LAGAN TENGAH KAB. TANJAB TIMUR SEBAGAI PEMBANGKIT LISTRIK. *J. Ilm. Univ. Batanghari Jambi* **13**, 1–23 (2013).
26. Saputra, V. H., Rifai, A. & Kunarso. Variabilitas musiman pola arus di perairan surabaya jawa timur. *J. Oceanogr.* **6**, 439–448 (2017). https://ejournal3.undip.ac.id/index.php/joce/article/view/20203
27. Fegie, I. N. & Sukojo, B. M. Identifikasi Sebaran Sedimentasi Dan Perubahan Garis Pantai Di Pesisir Muara Perancak-Bali Menggunakan Data Citra Satelit Alos

Avnir-2 Dan Spot-4. *Geoid* **9**, 73 (2013). https://doi.org/10.12962/j24423998.v9i1.747

28. Noor, D. *Geomorfologi*. (Deepublish, 2014).
29. Sari, T. A., Atmodjo, W. & Zuraida, R. STUDI BAHAN ORGANIK TOTAL (BOT) SEDIMEN DASAR LAUT DI PERAIRAN NABIRE, TELUK CENDRAWASIH, PAPUA. *J. OSEANOGRAFI* **3**, 81–86 (2014).
30. Hambali, R. & Apriayanti, Y. Studi Karakteristik Sedimen Dan Laju Sedimentasi Sungai Daeng. *J. Fropil* **4**, 165–174 (2016).
31. Ferguson, R. I. & Church, M. A simple universal equation for grain settling velocity. *J. Sediment. Res.* **74**, 933–937 (2004). https://doi.org/10.1306/051204740933
32. Gemilang, W. A., Wisha, U. J. & Rahmawan, G. A. Distribusi Sedimen Dasar Sebagai Identifikasi Erosi Pantai Di Kecamatan Brebes Menggunakan Analisis Granulometri. *J. Kelaut. Indones. J. Mar. Sci. Technol.* **10**, 54 (2017). https://doi.org/10.21107/jk.v10i1.2156
33. Hidayah, M. I. Dampak Pengembangan Reklamasi Terhadap Laju Sedimentasi dan Pola Arus di Kawasan Pantai Timur Surabaya (Pamurbaya). *Enviromental Sci.* (2017). http://repository.its.ac.id/45375/